Volume 5 | Issue 4 | 2025

ISSN | 2771-019X

Journal of
Clinical & Medical Images
Case Reports

Open Access |Research Article

Effects of stem cell exosomes and sanqi-derived exosome-like nanoparticles on oxidative stress in skin cells

***Corresponding Authors:** Xiaoting Zhang, Xiaomei Wang*

Email: Zhangxtcu@126.com; xmwang@szu.edu.cn

Xiaolu Yang[1#]; Ruiqi Yi[1#]; Ya Tian[2]; Aliza Fatima[5]; Umer Anayyat[1]; Fen Zhang; Hao Liu[4]; Zhuohang Yang[3]; Yi Ran[1]; Tangqin Zhang[1]; Xiaoting Zhang[2]*; Xiaomei Wang[1,2]

[1]*International Cancer Center, Shenzhen University Medical School, Shenzhen University, China.*

[2]*Songgang People's Hospital, China.*

[3]*School of Pharmacy, Shenzhen University Medical School, Shenzhen University, China.*

[4]*Shenzhen Shifangjie Technology Co., Ltd., China.*

[5]*Department of Biochemistry, University of Agriculture, Pakistan.*

Abstract

As the primary barrier against external damage, human skin is highly susceptible to oxidative stress, leading to cellular dysfunction. This study is the first to investigate the reparative effects and synergistic mechanisms of Mesenchymal Stem Cell-derived Exosomes (MSC-Exos) and Sanqi-derived Exosome-like Nanoparticles (SENs) on Hydrogen Peroxide (H_2O_2)-induced oxidative stress injury in Human Dermal Fibroblasts (HDFs). Experimental results demonstrated that both MSC-Exos and SENs were efficiently internalized by HDFs without significant cytotoxicity. While MSC-Exos alone markedly enhanced cell migration, SENs alone showed no pro-migratory effect. However, their combination synergistically promoted cell proliferation, significantly reduced intracellular Reactive Oxygen Species (ROS) levels, and restored mitochondrial membrane potential. Western blot analysis revealed that the combined treatment effectively suppressed apoptosis by upregulating the anti-apoptotic protein BCL-2 to pro-apoptotic protein BAX ratio. These findings indicate that MSC-Exos and SENs independently ameliorate H_2O_2-induced oxidative stress injury, with their combination exhibiting synergistic therapeutic potential.

Received: Jul 22, 2025

Accepted: Aug 14, 2025

Published Online: Aug 21, 2025

Cite this article: Yang X, Yi R, Tian Y, Zhang X, Wang X et al. Effects of stem cell exosomes and sanqi-derived exosome-like nanoparticles on oxidative stress in skin cells. J Clin Med Images Case Rep. 2025; 5(4): 1797.

Keywords: Mesenchymal stem cell exosomes (MSC-Exos); Sanqi exosome-like nanoparticles (SENs); Oxidative stress; Skin repair.

Introduction

As the largest organ and the body's first line of defense, the skin plays critical physiological roles in thermoregulation, sensory perception, and immune modulation [1,2]. Pathologically, ultraviolet radiation, inflammatory stimuli, viruses, and bacteria can elevate Reactive Oxygen Species (ROS) levels, inducing oxidative stress that triggers skin cell damage, including aging, necrosis, and apoptosis [3]. Although endogenous antioxidant systems counteract such damage, pathological conditions often disrupt redox homeostasis due to excessive ROS accumulation, overwhelming antioxidant defenses and exacerbating oxidative stress and inflammation [4,5]. Consequently, exogenous antioxidants hold promise for mitigating oxidative damage and promoting skin repair [6].

Exosomes, nanoscale extracellular vesicles secreted by cells, carry diverse bioactive molecules (proteins, lipids, and nucleic acids) and serve as key mediators of intercellular communication [7]. Their parent cell-mimetic biological functions make

exosomes a promising cell-free therapeutic strategy [8]. Mesenchymal Stem Cell-Derived Exosomes (MSC-Exos), in particular, exhibit potent anti-inflammatory, immunomodulatory, and tissue-regenerative properties [9], demonstrating therapeutic efficacy in cardiovascular diseases, neurological injuries, osteoarthritis, acute liver injury, diabetic wounds, and skin damage [10-16].

Beyond animal-derived exosomes, plant-derived Exosome-Like Nanoparticles (ELNs) have recently gained attention. Studies show that ELNs from plants such as grapefruit, ginger, strawberry, and cabbage are internalized by mammalian cells, exerting anti-inflammatory, antioxidant, and antimicrobial effects [17-21]. Panax notoginseng (Sanqi), a traditional Chinese herb, is widely studied for its hemostatic, antioxidant, and anti-inflammatory properties [22,23]. However, the role of Sanqi Exosome-like Nanoparticles (SENs) in mitigating skin oxidative stress remains unexplored.

This study investigates the reparative effects of MSC-Exos and SENs in an oxidative stress model. We treated H_2O_2-injured Human Dermal Fibroblasts (HDFs) with MSC-Exos and SENs, either alone or in combination, and evaluated their impacts on cell proliferation, ROS clearance, mitochondrial function, migration, and anti-apoptotic pathways.

Materials and methods

Preparation of MSC-Exos and SENs

Preparation for MSC-Exos: Collect the MSC culture supernatant and use the stem cell culture medium exosome extraction kit (Shifangjie S909) for the extraction of MSC-Exos. Place the collected MSC culture supernatant on ice, centrifuge at 6500g for 10 minutes to remove residual cells; collect the supernatant and centrifuge at 10000g for 10 minutes to remove cell debris. Transfer the supernatant to a new centrifuge tube and add Isolation Reagent A at a volume ratio of 2:1 (V-sample: V-A=2:1); invert and mix 3-5 times, then let it sit at 4°C for 5 minutes, followed by centrifugation at 13500 g for 3 minutes. Transfer the supernatant to a new centrifuge tube and add Isolation Reagent C at a volume ratio of 3:1; invert and mix 3-5 times, then let it sit at 4^{O}C for 1 hour, followed by centrifugation at 13500 g for 30 minutes. Discard the supernatant and collect the precipitate, which is the exosome; resuspend the precipitate in 500μL of physiological saline (or resuspension solution for downstream experiments) L of physiological saline (or resuspension solution for downstream experiments) according to subsequent experiments. Centrifuge the resuspended exosome solution at 5000 g for 10 minutes, discard the precipitate, and finally use the obtained exosomes for subsequent experiments or store them at -80^{O}C after aliquoting. (The refrigerated high-speed centrifuge used for centrifugation is Xiangyi H1580R.)

Preparation of SENs: First, clean and dry the Panax notoginseng, then extract the juice using the plant tissue liquid exosome extraction kit (Shifangjie S309) for the extraction of exosomes from Panax notoginseng. After collecting the plant tissue liquid, centrifuge at 10^{O}C at 6500 g for 10 minutes to remove residual plant tissue; collect the supernatant and centrifuge at 10000 g for 20 minutes to remove plant cell debris. Transfer the supernatant to a new centrifuge tube, add Isolation Reagent A at a volume ratio of 2:1 (V-sample: V-A=2:1); invert and mix 3-5 times, then let it sit at 4°C for 10 minutes, followed by centrifugation at 12000 g for 10 minutes. Transfer the supernatant to a new centrifuge tube and add Isolation Reagent C at a volume ratio of 3:1; invert and mix 3-5 times, then let it sit at 4^{O}C for 1 hour, followed by centrifugation at 13500 g for 0.5 hours. Discard the supernatant and collect the precipitate, which is the exosome; based on subsequent experiments, resuspend the precipitate in 500 μL of physiological L of physiological saline (or resuspension solution for downstream experiments). Centrifuge the resuspended exosome solution at 2000 g for 10 minutes, discard the precipitate, and finally use the obtained exosomes for subsequent experiments or store them at -80^{O}C after aliquoting. (The refrigerated high-speed centrifuge used for centrifugation is Xiangyi H1580R.)

Identification of MSC-Exos and SENs

BCA assay for exosomal samples: The exocytosis weight suspension was taken, and an equal volume of RIPA lysis solution (containing protease inhibitor) was added, and the sample was lysed at 4^{O}C for 1 h. The sample was completely lysed. Quantify the samples according to the BCA quantification kit instructions (Beyotime): standard solution: 0.5 mg/ml, add the standard in accordance with 0, 2, 4, 8, 12, 16, 20 μL to the standard of 96L to the standard of 96--well plate (repeated once per well), and well plate (repeated once per well), and add the standard dilution to replenish to 20 μLL, which is equivalent to the concentration of the standard of 0, 0.05, 0.1, 0.2, 0.3, respectively, 0.4, 0.5 mg/mL, add 20 μLL of sample to the 96-well plate (repeated once per well), add 200 μLL BCA working solution to each well, place at 37^{O}C for 20-30 min, measure the absorbance using an enzyme labeling instrument (Diatek DR3506), and calculate the protein concentration of the sample according to the standard curve and the sample volume used.

Measurement of exosome particle size concentration: Using the NTA particle size tracking analyzer (Malvern NS300), first of all, respectively, take the appropriate volume of exosomes diluted to the appropriate number of times, with the diluent to adjust the instrument to the optimal state, injected into the sample, particle size analysis and detection, until the sample to complete the detection of the instrument can be obtained to detect the exosomes of the particle size and concentration of information.

Transmission electron microscopy analysis of exosome samples: Using a projection electron microscope (Hitachi HT7700), the exosomes were firstly removed 50 μL; the sample L; the sample was aspirated 10 μL dropwise added to the copper mesh to precipitate for 1 min, and the floating liquid was sucked L dropwise added to the copper mesh to precipitate for 1 min, and the floating liquid was sucked off by the filter paper; dibasic uranium acetate 10 μL dropwise added to the cL dropwise added to the copper mesh to precipitate for 1 min, and the floating liquid was sucked off by the filter paper; and the exosomes were dried for a few minutes at room temperature, and the imaging was examined by electron microscopy at 100 kv, and the results of the transmission electron microscopy imaging were obtained.

Western blot of exosome samples: Western Blot was used to detect the expression of surface proteins of MSC-Exos and SENs. The protein concentration of the exosome was determined as shown in 2.2.1. 20 μg of g of protein was added to the buffer and boiled for 10 min. Prepare 12% separator gel and 5% concentrate gel. Add appropriate amount of electrophoresis solution and electrophoresis samples in an electrophoresis apparatus (Burroughs powerpac HC). Prepare transfer buffer and put the cut gel into it. Activate 0.22 mm PVDF membrane in metha-

nol, soak time is 30 seconds, lay the filter paper, membrane and gel in order, adjust the voltage 80V to transfer the membrane for 130 min. Take out the membrane and then put it on the shaking bed with sealing solution at 37+Cfor about 1.5 h. Primary antibody dilution was prepared for CD9, CD63 and STG101 antibody, put it on the shaking bed for sealing, 4^{O}C for 12-24 h. The membrane was washed with TBST for about 5-10min. The primary antibody was recovered after 4 washes with TBST for 5-10 min. 37^{O}C shakers for 2 h. The secondary antibody was incubated with horseradish enzyme labeled goat anti-rabbit IgG (1:5000). The membrane was washed with TBST for about 5-10 min/3-4 times and then visualized by chemiluminescence imaging using a gel imager (Tennant 4200).

Cell culture and processing

Human Dermal Fibroblasts (HDFs) were purchased from Wuhan Punosai Life Science and Technology Co. Cells were cultured in DMEM basal medium (Gibco) containing 10% Fetal Bovine Serum (FBS) (Gibco) and 1% penicillin-streptomycin double antibiotic solution (Gibco) at 37^{O}C and 5% CO_2 saturated humidity environment.

Cytotoxic effects of MSC-Exos and SENs

HDFs were inoculated into 96-well plates with 5000 cells per well of 100 mL, the plates were divided into two groups: a 24-hour group and a 48-hour group, each plate divided into blank control group, single MSC exosome group, single Sanqi exosome group, and mixed exosome group, with 5 replicate wells in each group. When the cell density was 80%-90%, exosomes were added according to different groups: in the single MSC exosome group and the single panax pseudoginseng exosome group, the final concentration of exosomes was 50 μg/mL; and in the mixed exosome group, the final concentration of MSC exosome and panax pseudoginseng exosome was 25 μg/mL each. 24 and 48 h of incubation, the reagent was prepared according to the instructions of the CCK8 kit (Beyotime), and was added to the plate, incubated for 1 h in a cell culture incubator at 37^{O}C and 5% CO_2. Incubate the plates in a cell culture incubator at 37^{O}C and 5% CO_2 for 1 h-2 h. Detect the absorbance value at 450 nm with an enzyme marker (BioTek), record the value and analyze statistically.

Exosome labeling

The HDFs were inoculated in 24-well plates, divided into blank control and hydrogen peroxide-treated groups, and the exosomes from MSC were labeled with PKH26 red fluorescent probe (Solarbio), and the exosomes from Panax quinquefolium were labeled with PKH67 green, fluorescent probe (Beijing Bio-

$$Cell\ \ viability(100\%) = \frac{A\ (drug-treated)\ -A\ (Blank)}{A\ (Control)\ -A\ (Blank)} \times 100\%$$

Lab Co., Ltd.). 200 μg of PKH26-labeled exosomes and PKH67-labeled exosomes were added into HDFs, cultured for 48 h, and then the cells were fixed with 4% paraformaldehyde (biosharp), and nuclear staining was carried out with DAPI staining solution (Beyotime), and the fluorescence signals of PKH26 and PKH67 were observed by the fully automated Intelligent Imaging System to analyze the relationship between cells and exosomes. The relationship between cells and exosomes was analyzed.

Cell proliferation assay

HDFs were inoculated into 96-well plates with 5000 cells per well of 100 mL, divided into blank control group, single H_2O_2-treated group, single MSC exosome group, single Sanqi exosome group, and mixed exosome group, with 5 replicate wells in each group. When the cell density was 80% and 90%, the cells were treated with medium containing 1 mM hydrogen peroxide for half an hour except for the blank control group, and then replaced with complete medium containing 10% FBS, and exosomes were added according to different groups: in the single

MSC exosome group and the single panax pseudoginseng exosome group, the final concentration of exosomes was 50 μg/mL; and in the mixed exosome group, the final concentration of MSC exosome and panax pseudoginseng exosome was 25 μg/mL each. 24 and 48 h of incubation, the reagent was prepared according to the instructions of the CCK8 kit, and was added to the plate, incubated for 1 h in a cell culture incubator at 37^{O}C and 5% CO_2. Incubate the plates in a cell culture incubator at 37^{O}C and 5% CO_2 for 1 h-2 h. Detect the absorbance value at 450 nm with an enzyme marker, record the value and analyze statistically.

Wound healing assay

HDF cells were seeded in a 24-well plate at a density of 3.5×10^4 cells per well with 1 mL per well, divided into a blank control group, a single H_2O_2 treatment group, a single MSC-Exos group, a single SENs group, and a mixed exosome group, with 2 replicates for each group. When the cell density reached 80%-90%, the cells in all groups except the blank control group were treated with a medium containing 1 mM hydrogen peroxide for half an hour. A pipette tip was used to create a scratch in the center of each well, ensuring the width of the scratch was consistent. The wells were then washed with PBS solution and replaced with complete medium containing 2% FBS. MSC-Exos and SENs were added according to the group (final concentration of 50 μg/mL), and the cells were incubated at 37^{O}C with 5% CO_2 for routine culture. Photos were taken at 0, 12, and 24 hours after scratching, and statistical analysis was performed.

Reactive oxygen species (ROS) generation detection

HDF cells were seeded in a 24-well plate at a density of 3.5×10^4 cells per well with 1 mL per well, divided into a blank control group, a single H_2O_2 treatment group, a single MSC-Exos group, a single SENs group, and a mixed exosome group, with 2 replicates for each group. When the cell density reached 80%-90%, the cells in all groups except the blank control group were treated with a medium containing 1 mM hydrogen peroxide for half an hour. The medium was replaced with complete medium containing 10% FBS, and MSC-Exos and SENs (final concentration of 50 μg /mL) were added according to the groups, and the cells were cultured for 48 h. The cells were labeled with ROS using Reactive Oxygen Detection Kit (Beyotime), and fluorescent probes 2',7'-Dichlorodihydrofluorescein Diacetate (DCFH-DA) to label ROS in the cells, incubate the cells at 37^{O}C, avoiding light for 30 min, and wash the cells twice with serum-free cell culture medium to fully remove the DCFH-DA that did not enter the cells, and take photos for observation using a fully automated intelligent imaging analysis system.

Mitochondrial membrane potential (MMP) Assay

The steps of cell grouping and oxidative stress modeling were the same as 2.6, using the mitochondrial membrane potential detection kit (JC-1) (Beyotime), adding JC-1 working solution 500 μL /well, incubating the cells for 30 L /well, incubating the cells for 30 min at 37^{O}C, avoiding light, washing twice with JC-1 buffer, and taking observation photos using the fully automated intelligent imaging analysis system.

Western blot

The steps of cell grouping and oxidative stress modeling were the same as in 2.4. After treatment, the cells were washed twice with PBS and the residual liquid was pipetted dry, and then lysed according to the ratio of high-efficiency RIPA lysate: protease inhibitor Cocktail (MedChemExpress)=10 mL:1 capsule, and the cells were lysed in six-well plates with 50 μL of the mixture in each well on ice, and then collected in EP tubes by a cell scraper L of the mixture in each well on ice, and then collected in EP tubes by a cell scraper and then centrifuged at 1000 rpm for 5 min. Proteins were collected in EP tubes using a cell spatula, followed by centrifugation at 1000 rpm for 5 min, heating at 100^{O}C dry thermostat (Hangzhou Ausheng Instrument Co., Ltd.) for 10 min, and subsequent cooling on ice for 10 min. Protein concentration was measured using the BCA Protein Assay Kit (ThermoFisher). Total proteins were mixed with 5× SDS-PAGE Protein Sampling Buffer (Beyotime), prepared to the same concentration, and heated to 100^{O}C for 10 min. Concentration gels and separation gels were prepared using a one-step PAGE Gel Rapid Preparation Kit (12.5%) (Yalase), and the concentration gels were prepared using a constant voltage current of 30 V and the separation gels were prepared using a constant voltage current of 90 V in 1x SWE Rapid HighSWE Rapid High--Resolution ElectrophoreResolution Electrophoresis Buffer (Wuhan Xavier Bio-Tech Co. Ltd.) to separate proteins. The proteins were separated in 1x iceice--bath free rapid membrane transfer buffer (Wuhan Xavier bath free rapid membrane transfer buffer (Wuhan Xavier Biotechnology Co., Ltd.) using a constant current of 400 mA to transfer the proteins to the PVDF membrane. After being closed with 5% skimmed milk for 2 h, the PVDF membranes were incubated with specific primary and secondary antibodies, and finally, the protein bands were visualized using an overly sensitive chemiluminescent agent in a fully automated chemiluminescent image analysis system (Tanon). The primary antibodies used included anti-Beta Actin (1:50 000, Wuhan Proteintech), BCL-2 (1:1 000, Wuhan Proteintech), BAX (1:1 000, Cell Signaling, USA), and the secondary antibodies used were Horseradish Peroxidase (HRP) and Horseradish Peroxidase (HRP). The secondary antibodies used were Horseradish Peroxidase (HRP)-coupled horse anti-mouse IgG (1:20 000, Cell Signaling, USA), HPR-coupled goat anti-rabbit IgG (1:20 000, Cell Signaling, USA), and Protein Marker (ThermoFisher).

Statistical analysis

All experiments were repeated at least 3 times. Western Blot images were processed using ImageJ software and data were processed using Prism 10 software, all data are expressed as Mean±SEM unless otherwise stated. Multiple comparisons were performed using one-way analysis of variance (ANOVA) if not otherwise indicated, and $P<0.05$ was considered a statistically significant difference.

Results

Characterization of MSC-Exos and SENs

Exosome is a cell-secreted nanoscale lipid bilayer membrane vesicle with a diameter of about 40-160 nm, which is approximated as a saucer-shaped or a hemisphere with one side concave under transmission electron microscope, and contains nucleic acids, proteins, lipids, and so on [24]. Based on the particle size, morphology and protein expression of the extracts can be identified as exosomes or not, the peak particle sizes of MSC-Exos and SENs extracted in this study were 124 nm and 90 nm, respectively (Figure 1A, Figure 1B), which were within the range of the particle size of exosomes. Under the electron microscope, both MSC-Exos and SENs were in the shape of “disk” or “cup”, and their diameters were around 100 nm (Figure 1C, Figure 1D), which was in line with the standard micromorphological characteristics of exosomes.

Fluorescent labeling and cellular uptake analysis of MSC-Exos and SENs

Both exosomes and plant-derived exosome-like nanoparticles have been shown to be efficiently delivered into mammalian cells [25,26]. To further validate the ability of fine HDF to take up MSC-Exos and SENs, MSC-Exos and SENs were labeled with PKH26 and PKH67, respectively, at a concentration of 25 μg/mL, and subsequently observed under a fluorescence microscope (Figure 2A). The green and red fluorescence within HDF indicate that MSC-Exos and SENs are able to be taken up by HDF.

Cytotoxic effects of MSC-Exos and SENs

To evaluate the cytotoxic effects of MSC-Exos and SENs on HDFs, cell viability was detected at 24 and 48 h after treatment in this study. The experimental results showed that neither MSC-Exos nor SENs exhibited cytotoxicity in the set concentration range. In addition, at 24h, SENs alone and in combination presented cell proliferation promotion, indicating that MSC-Exos and SENs not only have good biocompatibility, but also promote the proliferation of HDFs to a certain extent.

Effects of MSC-Exos and SENs on cell proliferation

The experiments showed that there was no significant difference in the cell proliferation levels among the experimental groups after 24 h treatment. However, after 48 h treatment, the cell proliferation level of the MSC-Exos and SENs combined group was significantly higher than that of the H_2O_2-treated group, whereas the experimental groups given MSC-Exos or SENs alone did not show statistically significant differences. This result suggests that under oxidative stress conditions, the combined action of MSC-Exos and SENs can more effectively promote the cell proliferation of HDFs and may have a synergistic protective effect.

Effects of MSC-Exos and SENs on cell migration

The cell scratch assay was used to observe the migration of HDFs related to wound healing. As shown in Figure 5, after 12h treatment, there was no significant difference in all groups compared to the H_2O_2-treated group, and there was a tendency to promote cell migration in the MSC-Exos group, but there was no statistical difference. After 24 h treatment, there was a statistically significant difference in the MSC-Exos group compared with the H_2O_2-treated group and the level of cell migration was similar to that of the blank control group; whereas, there was a tendency to promote cell migration in the MSC-Exos and SENs combination group although there was no statistically significant difference in the MSC-Exos and SENs combination group compared with the H_2O_2-treated group. It indicated that MSC-Exos could effectively promote the migration ability of HDFs under oxidative stress conditions, and the combination of MSC-Exos and SENs tended to promote the migration of HDFs.

Effects of MSC-Exos and SENs on reactive oxygen species generation and mitochondrial membrane potential

H_2O_2 induces cellular oxidative stress to damage HDFs, and the green fluorescence is the level of intracellular reactive oxy-

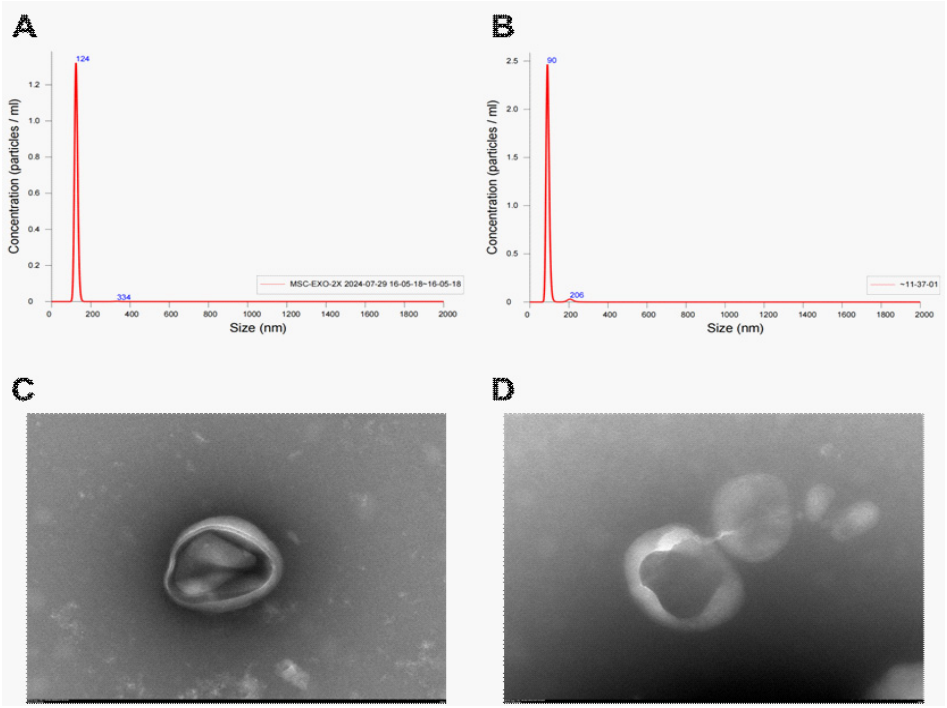

Figure 1: Exosome identification results. **(A,B)** Particle size analysis of MSC-Exos and SENs, respectively; **(C)** electron micrograph of MSC-Exos with a scale bar of 100 nm; **(D)** electron micrograph of SENs with a scale bar of 100 nm.

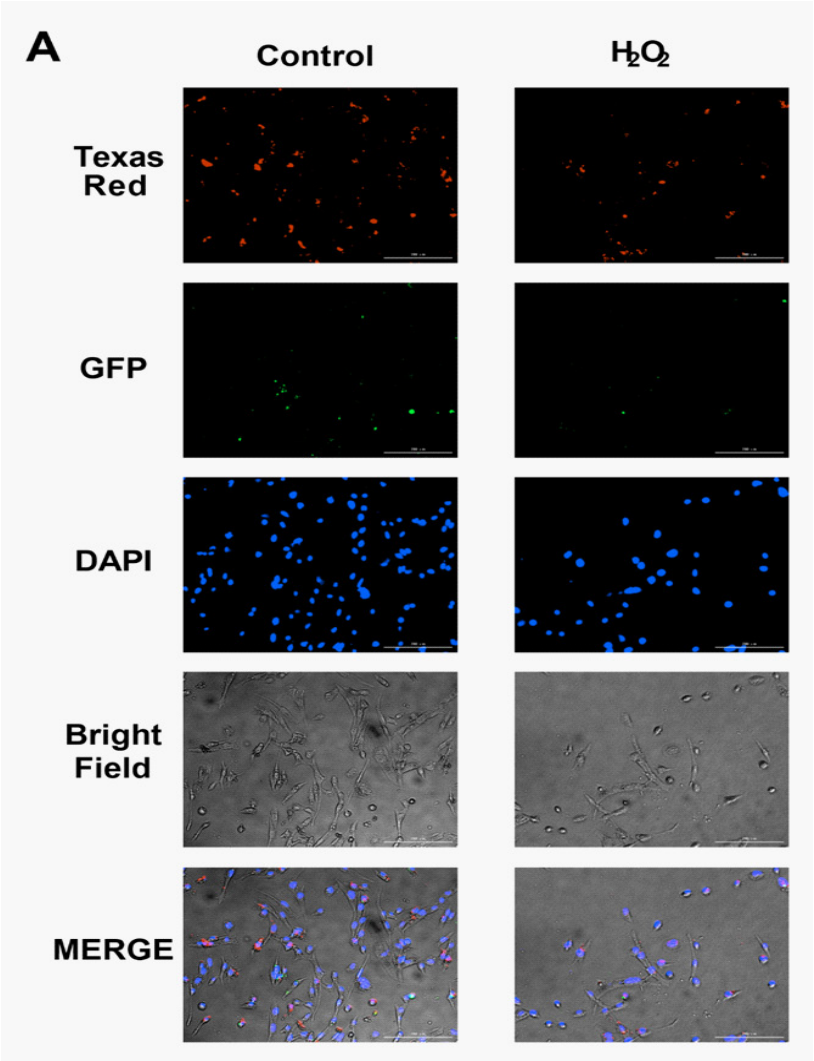

Figure 2: Uptake of MSC-Exos and SENs by HDFs. **(A)** MSC-Exos and SENs were stained with PKH26 and PKH67, respectively, and co-incubated with HDF for 48 h. Nuclei were stained with DAPI prior to visualization by fluorescence microscopy. The scale bar was 200μ m.

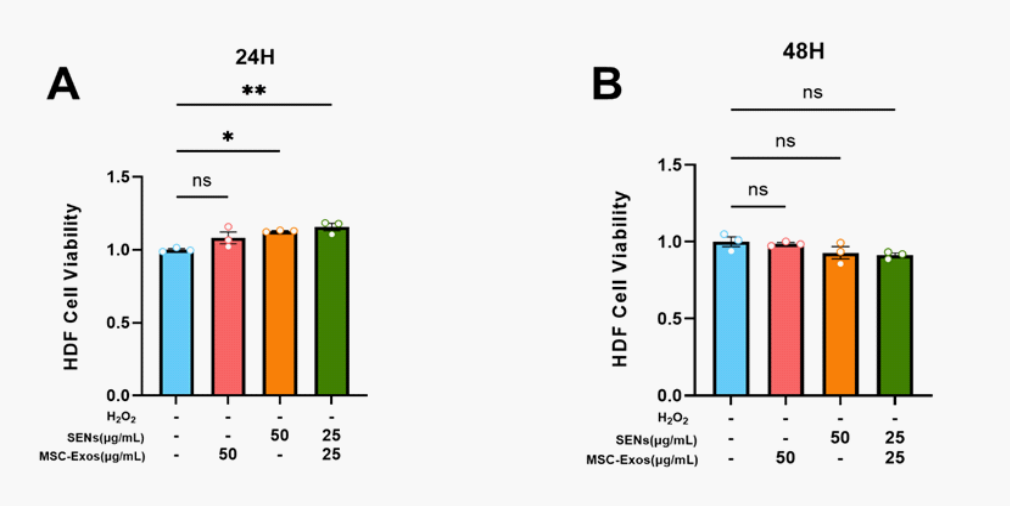

Figure 3: Cytotoxic effects of MSC-Exos and SENs. **(A,B)** Cell proliferation analysis by Cell Counting Kit-8 assay. absorbance was measured at 450 nm after 24 and 48 h of MSC-Exos and SENs treatment. (*p<0.05, **p<0.01, ns: not significant, n=3).

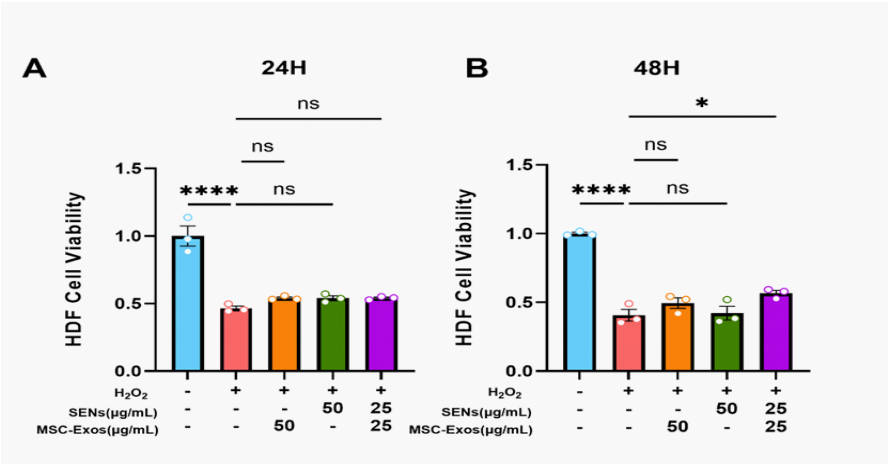

Figure 4: Effects of MSC-Exos and SENs on H_2O_2-induced oxidative stress model on cell proliferation. **(A,B)** Cell proliferation analysis by Cell Counting Kit-8 assay. 1 mM H_2O_2 was treated with 1 mM H_2O_2 for 0.5 h, followed by MSC-Exos and SENs for 24 and 48 h. Absorbance was measured at 450 nm. (*p<0.05, **** p<0.0001, ns: not significant, n=3)

gen species generation. The experiments showed that the average intracellular reactive oxygen species showed a decreasing trend after MSC-Exos and SENs treated oxidative stress HDFs for 48h, i.e., both exosomes

have obvious ROS scavenging ability, and the effect of the combination of MSC-Exos and SENs was more obvious (Figure 6A & 6C).

Under oxidative stress conditions, a decrease in mitochondrial membrane potential may lead to an increase in ROS generation, which in turn triggers apoptosis or autophagy. In this experiment, the mitochondrial membrane potential was detected using the JC-1 probe. When the mitochondrial membrane potential was high, JC-1 aggregated in the matrix of the mitochondria and formed a polymer, producing red fluorescence; when the mitochondrial membrane potential was low, JC-1 could not aggregate in the matrix of the mitochondria, and at this time, JC-1 was a monomer, producing green fluorescence. The experiments showed that the mitochondrial membrane potential level decreased significantly after H2O2 treatment of HDFs, and the mitochondrial membrane potential tended to increase after 48 h of treatment with MSC-Exos and SENs, and the increase was more obvious in the group of MSC-Exos and SENs in combination. This indicated that both MSC-Exos and SENs had the effect of restoring the mitochondrial membrane potential of oxidative stress cells, and the effect of MSC-Exos and SENs in combination was more obvious. (Figure 6B, Figure 6D).

Regulation of BAX and BCL-2 protein expression by MSC-Exos and SENs

Existing studies have shown that BCL-2 family proteins play a key role in the process of apoptosis through mitochondrial pathway [27]. Among them, BCL-2, as an anti-apoptotic protein, prevents the release of cytochrome C by inhibiting the permeability of the outer mitochondrial membrane, thereby maintaining the mitochondrial membrane potential. BAX, on the other hand, is a pro-apoptotic protein that initiates apoptosis by creating pores in the mitochondrial membrane that promote the release of cytochrome C [28]. Therefore, the ratio of BCL-2/BAX was positively correlated with the mitochondrial membrane potential level. The results showed that the ratio of BCL-2/BAX decreased significantly after H_2O_2 treatment of HDF, indicating that the mitochondrial membrane potential of H_2O_2 also decreased significantly, which was consistent with the change of

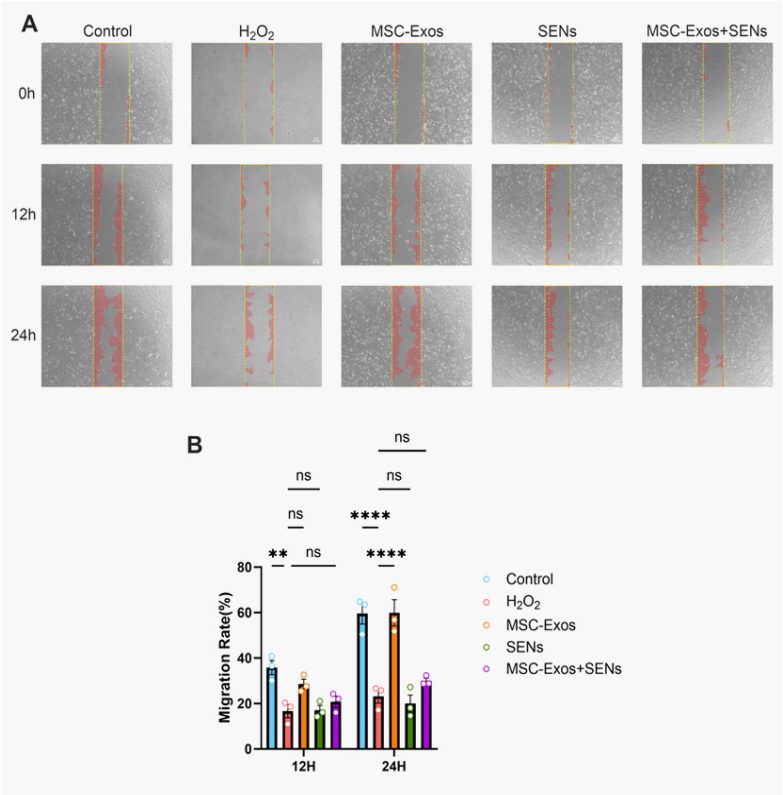

Figure 5: Effect of MSC-Exos and SENs on cell migration. **(A)** The cell scratch model was constructed and treated with 1 mM H_2O_2 for 0.5 h. After the treatment, MSC-Exos and SENs were added by group to verify the effect of exosomes on the migration effect of cells using the scratch assay. Scale bar was 40μ m; **(B)** Prism 10 analyzed Adobe Photoshop and ImageJ-treated images, and migration rates of scratched wounds were counted using two-factor ANOVA. (**p<0.01, ****p<0.0001,ns: not significant, n=3)

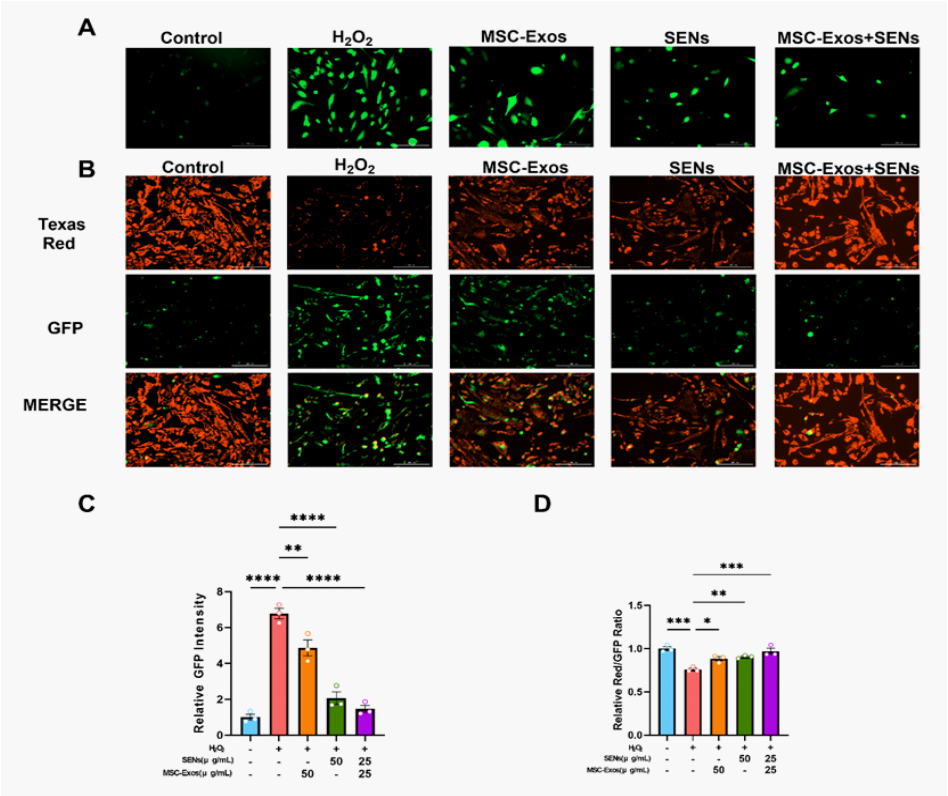

Figure 6: Effects of MSC-Exos and SENs on reactive oxygen species generation and mitochondrial membrane potential. **(A)** Levels of reactive oxygen species within HDFs were determined using DCFH-DA after treatment with 1 mM H_2O_2 for 0.5 h and treatment with MSC-Exos and SENs for 48 h. Scale bar is 200 μm; **(B)** Mitochondrial membrane potential within HDFs treated with MSC-Exos and SENs for 48 h after 0.5 h treatment with 1 mM H_2O_2 was determined using JC-1. Scale bar is 200 μm; **(C)** Relative fluorescence intensity of ROS was analyzed using Prism 10; **(D)** Relative ratio of red fluorescence to green fluorescence was analyzed using Prism 10. (*p<0.05, **p<0.01, ***p<0.001,****p<0.0001, ns: not significant, n=3).

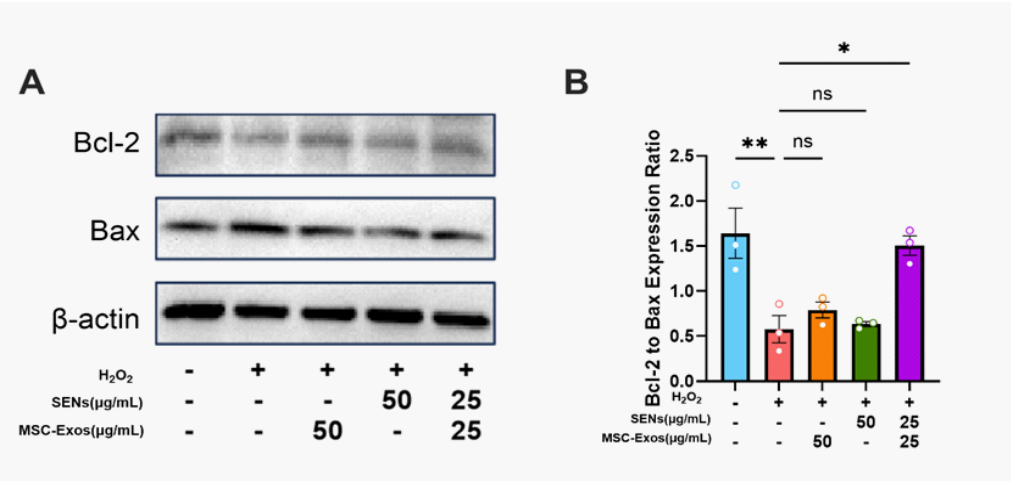

Figure 7: Regulation of BAX and BCL-2 protein expression by MSC-Exos and SENs. **(A)** Expression of BCL-2, BAX, and β- Actin within treated HDFs; **(B)** Ratio of BCL-2/BAX in each group after quantitative analysis by Image J. (*p<0.05, **p<0.01, ns: not significant, n=3).

mitochondrial membrane potential of 3.6, and the ratio of BCL-2/BAX increased after 48 h of MSC-Exos and SENs treatment, and was more obvious in the SC-Exos and SENs group, which was also consistent with the experimental results of 3.6. These results indicated that the combination of MSC-Exos and SENs could promote the expression of BCL-2, thereby maintaining the mitochondrial membrane potential level and exerting anti-apoptotic effects. At the same time, the expression of BAX decreased, indicating that the combination of MSC-Exos and SENs could inhibit the production of pro-apoptotic signals, thereby inhibiting apoptosis (Figure 7).

Discussion

Oxidative stress has been implicated in a variety of pathological processes, such as skin aging, chronic inflammatory skin diseases, and delayed healing from trauma [29,30]. Among them, ROS is a key mediator of cell signaling pathways and inflammation during healing [31]. Excessive oxidative stress caused by ROS overproduction after trauma can lead to cellular senescence, apoptosis, and chronic inflammation, ultimately interfering with wound healing process [31]. In addition, mitochondria are the main source of intracellular ROS, and their functional status is of great significance for the maintenance of cellular redox homeostasis [32]. However, under conditions of oxidative stress, excessive levels of ROS can disrupt the integrity of mitochondrial membranes, leading to mitochondrial dysfunction and cell damage [32,33].

Oral administration of exogenous antioxidants in everyday life can be considered a traditional means of antioxidant, but these treatments often fail to achieve the desired antioxidant effect due to the first-pass effect [34,35]. In recent years, stem cell exosomes and plant-derived exosome-like nanoparticles have attracted extensive attention due to their good biocompatibility, drug loading capacity, and potential to modulate cell function [36,37]. Therefore, in this study, H_2O_2-induced oxidative stress model was used to explore the role and synergistic effect of MSC-Exos and SENs in damage repair.

The results showed that both MSC-Exos and SENs were efficiently taken up by HDF cells (Figure 2), which is consistent with previous studies [25,26]. Moreover, the intracellular distribution of the two is not fused with each other (Figure 2), suggesting that they can enter the cell as independent functional units to play a role. This phenomenon may be related to differences in membrane composition and surface proteins between mammalian exosomes and plant-derived nanoparticles [38]. This "independent" pattern of uptake may be beneficial for each of its specific biological functions.

In functional experiments, we observed that both exosomes were non-cytotoxic and even promoted HDF proliferation at some concentrations and time points (Figure 3), showing good biocompatibility. MSC-Exos significantly enhanced cell migration in scratch assays, while SENs alone did not exhibit a migration-promoting effect. The role of MSC-Exos in promoting cell migration may be related to its abundance of growth factors and regulatory miRNAs. MiR-21-5p and miR-125b-5p, among others, have been shown to promote fibroblast migration and inhibit scarring [39,40]. In contrast, the migration-promoting effect of SENs in this study was not significant, which may be due to the fact that the components of SENs are more inclined to antioxidant and anti-inflammatory, rather than directly activating migration-related signaling pathways, but this still needs to be verified experimentally.

From the perspective of mechanism, exosome combination can significantly reduce the level of intracellular ROS, restore mitochondrial membrane potential, and upregulate the BCL-2/BAX ratio, suggesting that it can achieve antioxidant and pro-survival effects by stabilizing mitochondrial function and inhibiting mitochondria-related apoptosis pathways. It is worth noting that although SENs did not significantly promote cell migration, they performed prominently in regulating ROS clearance and mitochondrial function, suggesting that they may be used as a powerful supplement to enhance the antioxidant effect of stem cell exosomes.

The advantage of this study is that it is the first time to propose and verify the synergistic antioxidant strategy of plant-derived exosome-like nanoparticles and stem cell exosomes, which provides a new research idea for the combined application of multi-source exosomes in skin injury repair. However, there are still some limitations in this study, for example, the specific bioactive components of SENs have not yet been clarified, and the composition analysis in exosomes still needs to be deepened. In addition, this study is an in vitro study, and further animal models and tissue repair experiments are needed in the future to verify its application prospect in real skin trauma environments.

Conclusion

This study showed that both MSC-Exos and SENs could improve H_2O_2-induced oxidative stress damage, and MSC-Exos played a significant role in promoting cell migration, while SENs mainly played an antioxidant role. The combination of the two has a synergistic effect in promoting cell proliferation, reducing ROS level, restoring mitochondrial membrane potential and regulating the BCL-2/BAX ratio, which provides a new research direction for the combined application of exosomes.

Declarations

Authorship contribution statement: Xiaolu Yang: experimental research, data analysis, paper writing. Ruiqi Yi: experimental research, data analysis, paper writing. Aliza Fatima: data organization and revision. Umer Anayyat: data organization, paper revision and editing. Fen Zhang: MSC-Exos extraction and characterization. Hao Liu: SENs extraction and characterization. Zhuohang Yang: literature search, data proofreading. Yi Ran: Literature search, data proofreading. Tangqin Zhang: data organization. Xiaomei Wang: research guidance, financial support, thesis review.

Conflict of interest: The authors declare that the publication of this article has no conflicts of interest.

Funding: This research was funded by Shenzhen Science and Technology Program (No. JCYJ20230807151000002).

Data availability: Requests to access the datasets of this study should be directed to Xiaomei Wang.

References

1. Zhang Y, Zheng Z, Zhu S, Xu L, Zhang Q, Gao J, et al. Electroactive electrospun nanofibrous scaffolds: innovative approaches for improved skin wound healing. Adv Sci. 2025; 2416267.
2. Zhong Y, Wei E, Wu L, Wang Y, Lin Q, Wu N, et al. Novel biomaterials for wound healing and tissue regeneration. ACS Omega. 2024; 9: 32268-86.
3. Liu HM, Tang W, Lei SN, Zhang Y, Cheng MY, Liu QL, Wang W. Extraction optimization, characterization and biological activities of polysaccharide extracts from Nymphaea hybrid. Int J Mol Sci. 2023; 24: 8974.
4. Israni DK, Raghani NR, Soni J, Shah M, Prajapati BG, Chorawala MR, et al. Harnessing Cannabis sativa oil for enhanced skin wound healing: the role of reactive oxygen species regulation. Pharmaceutics. 2024; 16: 1277.
5. Ricci A, Stefanuto L, Gasperi T, Bruni F, Tofani D. Lipid nanovesicles for antioxidant delivery in skin: liposomes, ufasomes, ethosomes, and niosomes. Antioxidants (Basel). 2024; 13: 1516.
6. Brand RM, Wipf P, Durham A, Epperly MW, Greenberger JS, Falo LD. Targeting mitochondrial oxidative stress to mitigate UV-induced skin damage. Front Pharmacol. 2018; 9: 920.
7. Yu H, Feng H, Zeng H, Wu Y, Zhang Q, Yu J, et al. Exosomes: the emerging mechanisms and potential clinical applications in dermatology. Int J Biol Sci. 2024; 20: 1778-95.
8. Zhou C, Zhang B, Yang Y, Jiang Q, Li T, Gong J, et al. Stem cell-derived exosomes: emerging therapeutic opportunities for wound healing. Stem Cell Res Ther. 2023; 14: 107.
9. Gong X, Zhao Q, Zhang H, Liu R, Wu J, Zhang N, et al. The effects of mesenchymal stem cells-derived exosomes on metabolic reprogramming in scar formation and wound healing. Int J Nanomedicine. 2024; 19: 9871-87.
10. Wang Z, Zhong D, Yan T, Zheng Q, Zhou E, Ye Z, et al. Stem cells from human exfoliated deciduous teeth-derived exosomes for the treatment of acute liver injury and liver fibrosis. ACS Appl Mater Interfaces. 2025; 17: 17948-64.
11. Wang Z, Xu H, Xue B, Liu L, Tang Y, Wang Z, et al. MSC-derived exosomal circMYO9B accelerates diabetic wound healing by promoting angiogenesis through the hnRNPU/CBL/KDM1A/VEGFA axis. Commun Biol. 2024; 7: 1700.
12. Wu H, Hui Y, Qian X, Wang X, Xu J, Wang F, et al. Exosomes derived from mesenchymal stem cells ameliorate impaired glucose metabolism in myocardial ischemia/reperfusion injury through miR-132-3p/PTEN/AKT pathway. Cell Cycle. 2025; 1-20.
13. Zi Y, Li J, Qian X, Li J, Jin Y, Zhang Z, et al. Human umbilical cord mesenchymal stem cell exosomes promote elastin production and acute skin wound healing via TGFβ1-Smad pathway. Mol Cell Biochem. 2025.
14. Molecular events in MSC exosome mediated cytoprotection in cardiomyocytes. Sci Rep. 2019.
15. Fu Y, Cui S, Zhou Y, Qiu L. Dental pulp stem cell-derived exosomes alleviate mice knee osteoarthritis by inhibiting TRPV4-mediated osteoclast activation. Int J Mol Sci. 2023; 24: 4926.
16. Liu M, Li H, Xiong G, Zhang B, Zhang Q, Gao S, et al. Mesenchymal stem cell exosomes therapy for the treatment of traumatic brain injury: mechanism, progress, challenges and prospects. J Transl Med. 2025; 23: 427.
17. Chen X, Xing X, Lin S, Huang L, He L, Zou Y, et al. Plant-derived nanovesicles: harnessing nature's power for tissue protection and repair. J Nanobiotechnology. 2023; 21: 445.
18. Kumar A, Sundaram K, Teng Y, Mu J, Sriwastva MK, Zhang L, et al. Ginger nanoparticles mediated induction of Foxa2 prevents high-fat diet-induced insulin resistance. Theranostics. 2022; 12: 1388-403.
19. Perut F, Roncuzzi L, Avnet S, Massa A, Zini N, Sabbadini S, et al. Strawberry-derived exosome-like nanoparticles prevent oxidative stress in human mesenchymal stromal cells. Biomolecules. 2021; 11: 87.
20. Sundaram K, Miller DP, Kumar A, Teng Y, Sayed M, Mu J, et al. Plant-derived exosomal nanoparticles inhibit pathogenicity of Porphyromonas gingivalis. iScience. 2019; 21: 308-27.
21. Savcı Y, Kırbaş OK, Bozkurt BT, Abdik EA, Taşlı PN, Şahin F, et al. Grapefruit-derived extracellular vesicles as a promising cell-free therapeutic tool for wound healing. Food Funct. 2021; 12: 5144-56.
22. Zhao C, Wu S, Wang H. Medicinal plant extracts targeting UV-induced skin damage: molecular mechanisms and therapeutic potential. Int J Mol Sci. 2025; 26: 2278.
23. Mo Y, He X, Cui H, Cheng Y, Zhou M, Cui X, et al. Gut microbiota: a new key of understanding for Panax notoginseng against multiple disorders and biotransformation. J Ethnopharmacol. 2025; 341: 119306.
24. He C, Zheng S, Luo Y, Wang B. Exosome theranostics: biology and translational medicine. Theranostics. 2018; 8: 237-55.
25. Mulcahy LA, Pink RC, Carter DRF. Routes and mechanisms of extracellular vesicle uptake. J Extracell Vesicles. 2014; 3: 24641.
26. Chu K, Liu J, Zhang X, Wang M, Yu W, Chen Y, et al. Herbal medicine-derived exosome-like nanovesicles: a rising star in cancer therapy. Int J Nanomedicine. 2024; 19: 7585-603.
27. Singh R, Letai A, Sarosiek K. Regulation of apoptosis in health

and disease: the balancing act of BCL-2 family proteins. Nat Rev Mol Cell Biol. 2019; 20: 175-93.

28. Renault TT, Dejean LM, Manon S. A brewing understanding of the regulation of Bax function by Bcl-xL and Bcl-2. Mech Ageing Dev. 2017; 161: 201-10.

29. Nakai K, Tsuruta D. What are reactive oxygen species, free radicals, and oxidative stress in skin diseases? Int J Mol Sci. 2021; 22: 10799.

30. Salman S, Paulet V, Hardonnière K, Kerdine-Römer S. The role of NRF2 transcription factor in inflammatory skin diseases. Biofactors. 2025; 51: e70013.

31. Oh GW, Kim SC, Cho KJ, Ko SC, Lee JM, Yim MJ, et al. Poly(vinyl alcohol)/chitosan hydrogel incorporating chitooligosaccharide-gentisic acid conjugate with antioxidant and antibacterial properties as a potential wound dressing. Int J Biol Macromol. 2024; 255: 128047.

32. Martins AC, Oliveira-Paula GH, Tinkov AA, Skalny AV, Tizabi Y, Bowman AB, et al. Role of manganese in brain health and disease: focus on oxidative stress. Free Radic Biol Med. 2025; 232: 306-18.

33. Wei F, Gu W, Zhang F, Wu S. Paralysis caused by dinotefuran at environmental concentration via interfering the Ca2+-ROS-mitochondria pathway in Chironomus kiiensis. Front Public Health. 2024; 12: 1468384.

34. Xia Y, Li X, Huang F, Wu Y, Liu J, Liu J. Design and advances in antioxidant hydrogels for ROS-induced oxidative disease. Acta Biomater. 2025; 194: 80-97.

35. Xue Y, Wang T, Liu JP, Chen Q, Dai XL, Su M, et al. Recent trends in the development and application of nano-antioxidants for skin-related disease. Antioxidants (Basel). 2024; 14: 27.

36. Han Y, Guo X, Ji Z, Guo Y, Ma W, Du H, et al. Colon health benefits of plant-derived exosome-like nanoparticles via modulating gut microbiota and immunity. Crit Rev Food Sci Nutr. 2025; 1-21.

37. Kalluri R, LeBleu VS. The biology, function, and biomedical applications of exosomes. Science. 2020; 367: eaau6977.

38. Yi C, Lu L, Li Z, Guo Q, Ou L, Wang R, et al. Plant-derived exosome-like nanoparticles for microRNA delivery in cancer treatment. Drug Deliv Transl Res. 2025; 15: 84-101.

39. Gowtham A, Kaundal RK. Exploring the ncRNA landscape in exosomes: insights into wound healing mechanisms and therapeutic applications. Int J Biol Macromol. 2024; 292: 139206.

40. Zhang Y, Pan Y, Liu Y, Li X, Tang L, Duan M, et al. Exosomes derived from human umbilical cord blood mesenchymal stem cells stimulate regenerative wound healing via transforming growth factor-β receptor inhibition. Stem Cell Res Ther. 2021; 12: 434.